Arab J. Nucl. Sci. Appl., Vol. 57, 4, 68-86 (2024)

ISSN 1110-0451

Arab Journal of Nuclear Sciences and Applications

Web site: ajnsa.journals.ekb.eg

(E S N S A)

Fast and Accurate Detection and Classification of Kidney Diseases from CT Images using Hybrid Classifiers

Wessam S. ElAraby, Ehab H. El-Shazly* and Mohamed H. Saad*

Radiation Engineering Department, National Center for Radiation Research and Technology (NCRRT), Egyptian Atomic Energy Authority, Cairo 11787, Egypt.

ARTICLE INFO

Article history:

Received: 18th Aug. 2024

Accepted: 16th Sept. 2024

Available online: 1st Oct. 2024

Keywords:

Nephrolithiasis, Kidney Diseases;

Convolution Neural Network;

Medical CT Images;

Support Vector Machine

ABSTRACT

This research introduces an innovative method of Artificial Intelligence (AI) for improving the detection and classification of kidney diseases using CT images. The proposed method includes image pre-processing to remove artifacts, noise, and other image quality issues that can affect the accuracy of diagnosis. Then the area of interest in each image is segmented using Fractional Darwinian particle swarm optimization. Different features including Local Binary Pattern, Hu Moments, and Gray level zone length matrix (GLZLM) are extracted and fused using Canonical Correlation Analysis (CCA) and reduced using Two Dimensional Principal Component Analysis (2D- PCA) to maintain only dominant features. A two-level classification approach is carried out to provide both fast and detailed diagnosis using both Binary Support Vector Machine (BSVM) and Convolutional Neural Network (CNN) in sequence. BSVM is used to initially discriminate between normal and abnormal kidney states. Afterwards, the detected abnormal kidney images are classified using CNN to different kidney diseases such as stones, cysts, and tumors. This approach aims to expedite the diagnostic procedure while also enhancing the efficiency and accuracy of classifying kidney disease in the clinical practice. Obtained results validate the efficiency of our proposed in terms of achieved accuracy when compared to alternative cutting-edge methods.

1. INTRODUCTION

Computed tomography (CT) gives extensive information about the kidneys' internal anatomy for the diagnosis and management of renal diseases. Kidney diseases, such as kidney stones, cysts, and tumors, are serious health issues that impact millions of people worldwide. However, radiologists' manual interpretation of CT scans takes time and is subjective, which can lead to diagnostic mistakes. As a result, automated approaches are needed to detect and classify renal diseases in CT scans.

Artificial intelligence (AI) offers a multitude of tools to improve our lives and has had substantial effects in several domains, such as the medical industry [1]. AI has greatly assisted in the prompt detection, diagnosis, and treatment of diseases in the medical domain. Currently, kidney illness stands as a prominent worldwide health concern. Although there is a high prevalence of people with renal disease, diagnosing and treating this condition continues to be difficult. Currently, there are AI-based diagnostic methods that take into account individual situations and are capable of making appropriate conclusions. These advancements have great potential for making considerable progress in the field of renal disease diagnosis [2, 3].

Both traditional machine learning approaches and deep learning techniques have been recently utilized for the identification and categorization of kidney diseases in CT images. Traditional machine learning approaches, such as the support vector machine (SVM), have been used to classify kidney stones [4] and malignancies [5], resulting in high accuracy. However, these approaches cannot take full advantage of the abundant information in CT scans. On the other hand, Convolutional Neural Networks (CNNs) have been proven to be an efficient

Corresponding author (s) E-mail(s): ehab.elshazly@ejust.edu.eg, m.hassansaad@gmail.com;

DOI: 10.21608/AJNSA.2024.313417.1841

for medical image processing applications, including the identification and categorization of kidney diseases in CT images [6, 7]. CNNs may learn hierarchical characteristics from images leading to enhanced performance. Nevertheless, CNNs are characterized by their high computing demands and may not be appropriate in situations when quick decision-making is necessary.

To overcome these constraints, in this research, we present a hybrid classifier built of BSVM-CNN for the speedy and exact identification and categorization of kidney diseases in CT images. The suggested approach utilizes a two-step classification procedure: in the initial stage, a binary support vector machine (BSVM) is employed to swiftly determine if kidney images are normal or infected. If the image is detected as having diseases, then it is transmitted to the second stage judgment, which applies CNN, to differentiate

between different kidney diseases (stones, cysts, and tumors). The suggested technique seeks towards improving the accuracy and efficiency of kidney illness identification and categorization in CT images, hence facilitating early diagnosis and treatment of renal diseases. Our contributions to obtain the best performance in respect to the lowest time and fastest decision might be stated as follows:

1- A robust approach for image segmentation using Fractional Darwinian Particle Swarm Optimization (FDPSO) is proposed. Fractional calculus optimizes the performance by adjusting the convergence rate, delivers more accurate segmentation results, and is more resilient to noise than classic thresholding approaches.

2- Multiple characteristics for texture and form analysis such as Local Binary Patterns (LBP), GLZLM, and Hu Moments are extracted and fused together using Canonical Correlation Analysis (CCA.(

3- Dimensionality reduction of the feature space is achieved using Two- Dimensional Principal Component Analysis (2DPCA) to enhance the performance of the classifier by allowing for easier visualization and potentially capturing the most important information in the data.

4- Improved efficiency and accuracy of kidney disease detection and classification supports clinicians in their clinical practice using a hybrid classifier approach that uses a binary Support Vector Machine (SVM) for fast decision-making and a Convolutional Neural Network (CNN) for further classification.

5- A detailed examination of the suggested strategy on a large data set of CT scans, revealing its superiority over current methods in terms of accuracy, sensitivity, and specificity.

The remaining part of the paper is arranged as follows. Section 2 examines the relevant work to set the basis for introducing our intended study. Section 3 discusses our intended work in depth. Section 4 outlines the experimental setup while the lengthy experiments and the findings produced are presented in section 5. Section 6 draws conclusions.

2. RELATED WORK

Recent advancements in computer vision have propelled AI-based algorithms to the forefront of kidney disease diagnosis. This growing interest is driven by their effectiveness in detecting various conditions. Researchers have developed numerous approaches for kidney disease diagnosis using machine learning (ML) and convolutional neural networks (CNNs.(

In [8], the authors explored ML techniques to create effective tools for predicting Chronic Kidney Disease (CKD). Their approach includes class balancing to address the uneven distribution of instances between classes, ranking of features and analysis, and the training of several ML models evaluated using various performance metrics. The results revealed that the Rotation Forest.

(RotF) model excelled, getting an Area Under the Curve (AUC) of 100%, and illustrating precision, recall, F-measure, and accuracy rates of 99.2%.

In [9] the authors applied eight different ML algorithms for building a system for the rapid diagnosis of CKD. The algorithms used include Extra Trees Classifier (EXT), K-Nearest Neighbors (KNN), AdaBoost (ADB), Extreme Gradient Boosting (XGB), Gradient Boosting (GB), Gaussian Naïve Bayes (GNB), Decision Tree (DT), and Random Forest (RF). Among these, KNN and Extra Trees classifiers demonstrated the highest accuracy, at 99% and 98%, respectively.

In [10], the authors proposed a method for kidney problem detection using smartphone images from ultrasound scanners. The approach employs the Viola-Jones method for initial detection, followed by texture feature extraction and classification with a Support Vector Machine (SVM). This method achieved an accuracy of 90.91

Moreover, [11] presented an algorithm for detecting Nephrolithiasis using KNN and SVM techniques. The study enhances image quality through median filtering and unsharp masking, with Gaussian and Median filters used for further processing. Erosion and dilation operations, along with entropy-based segmentation, are employed to define the region of interest. The combination of KNN and SVM classifiers resulted in an accuracy of 85%.

In [12], a pre-processing approach involving grey-scale conversion, region- of-interest definition, and feature extraction using a multi-scale wavelet-based Gabor method is utilized. Optimization is performed using Cuckoo Search (CS), while classification is carried out utilizing an Artificial Neural Network (ANN). This approach produced a classification accuracy of 94%.

Furthermore, [13] defined three regions of interest (ROIs) in kidney ultra- sound images: the cortex, the boundary between the cortex and medulla, and the medulla. The study used the Gray Level Co-occurrence Matrix (GLCM) technique to extract 57 parameters from these ROIs, augmented with kidney size information, totaling 58 features. An ANN model with 58 input parameters, 10 layers that are hidden, and 3 layers of output (representing normal, mild, moderate, and severe CKD) achieved a classification rate of 95.4%.

In [14], a predictive approach for CKD status is presented, incorporating data pre-processing, handling of missing values, feature extraction, and data aggregation. The study applies several ML techniques, including logistic regression (LR), DT classification, and KNN, with LR achieving the highest accuracy of approximately 97%.

Lastly, [15] outlined a four-phase approach to kidney stone detection. Challenges such as speckle noise and poor contrast are addressed through appropriate image processing techniques. Gaussian filtering is used for noise reduction, followed by Canny edge detection for segmentation. The segmented image is subsequently analyzed using wavelet transforms and CNN classification to identify kidney stones.

3 PROPOSED WORK

Fig. 1 shows the flowchart of our proposed Kidney Nephrolithiasis detection using Binary and multi class classification techniques: First, Binary classification between normal and abnormal kidney images is made using binary SVM, then, multi class classification among different kidney diseases is made using CNN. The next subsections explain in detail each step in our proposed approach.

3.1 Image Pre-processing

CT kidney medical images usually contain artifacts, noise, and other image quality issues that can affect the accuracy of diagnosis and analysis. Therefore, image pre-processing is an essential step that is being used to enhance the quality of these images by eliminating such artifacts, reducing noise, and improving contrast. Samples of the enhanced images data set are shown in Fig. 2.

The implementation of various image pre-processing techniques plays a crucial role in significantly boosting the accuracy, dependability, and overall quality of medical diagnoses and analyses. This, in turn, leads to improved patient outcomes, ensuring that individuals receive more effective and precise medical care. The process of preparing computed tomography (CT) kidney image data sets for subsequent analysis involves a series of essential operations and steps. These pre-processing steps are designed to optimize the image quality and make the data more suitable for analysis. Some of these important pre-processing techniques include the following operations:

1. Noise Reduction: CT images often suffer from high noise levels due to factors like scanner hardware, patient motion, or radiation dose, which can compromise image quality and analytical accuracy. Employing noise reduction algorithms, such as Gaussian or median filters, can enhance image quality by smoothing the image through averaging pixel values in the surrounding area, thus mitigating random noise.

2. Contrast Enhancement: CT images often exhibit poor contrast, complicating the differentiation of various tissue types. Techniques like histogram equalization and adaptive histogram equalization can enhance this contrast. Histogram equalization redistributes pixel intensities for a uniform distribution, while adaptive histogram equalization applies this locally in smaller regions. These methods improve the visibility of kidney structures.

3. CT images often contain irrelevant elements, such as the scanner bed or extraneous body parts. Cropping these images to focus on the area of interest reduces computational load and improves model accuracy. Resizing to a standard resolution further standardizes the data, making it more suitable for training machine learning algorithms that require consistent image sizes.

4. Normalization is a technique that ensures a consistent distribution of image intensities, which is beneficial for machine learning algorithms that assume specific data properties, like a Gaussian distribution. During this process, the mean pixel value is subtracted from each pixel then divided by the standard deviation, resulting in pixel values with a mean of zero and a standard deviation of one.

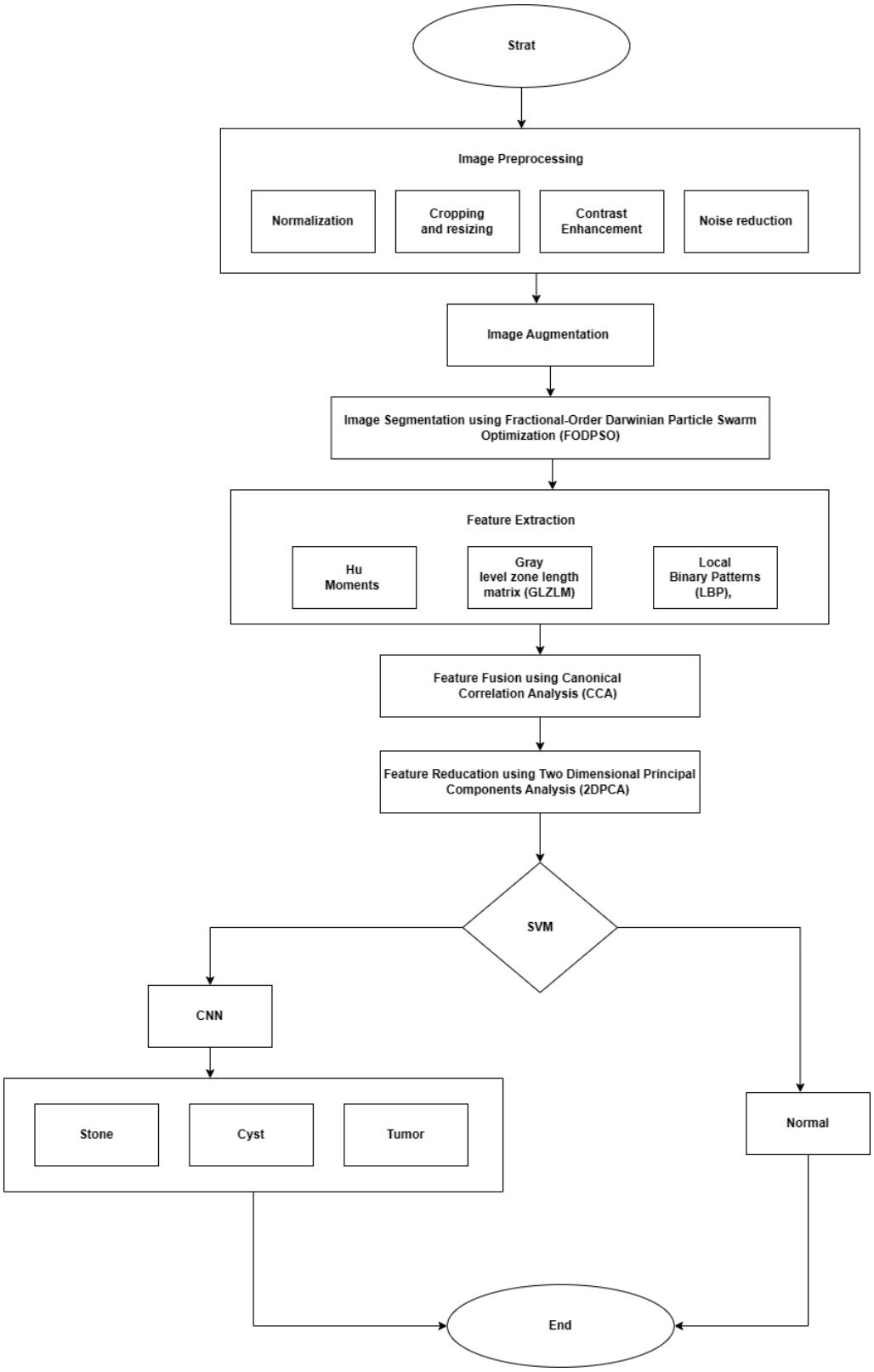

Fig. (1): Flowchart for the proposed Kidney Nephrolithiasis Detection approach

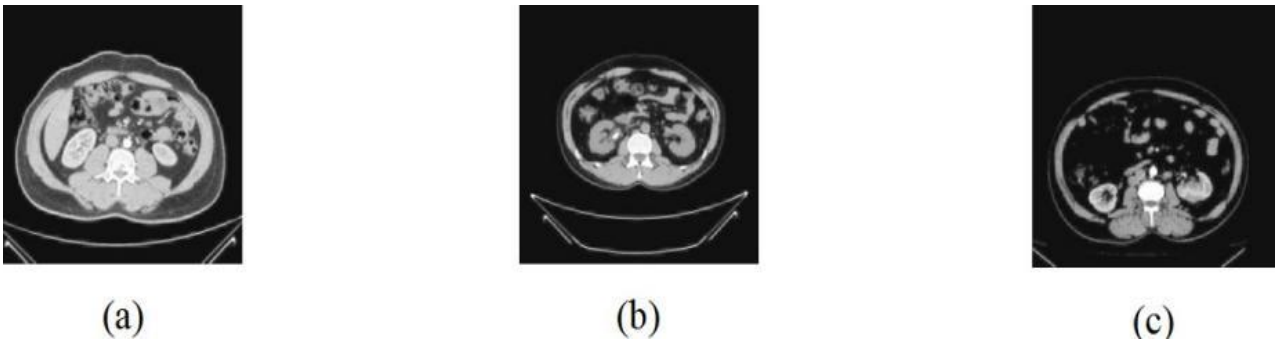

Fig. (2): Sample of the images data set after enhancements: (a) Normal, (b) Kidney Stone, and (c) Tumor

Table (1): Number of new instances generated after data augmentation step for each class

	Before Data Augmentation	After Data Augmentation	New Instances Generated
Cyst	3709	10527	6818
Normal	5077	14308	9231
Stone	1377	3885	2508
Tumor	2283	6443	4160
Total	12446	35163	22717

3.2 Image Augmentation

Image augmentation for X-ray kidney images includes transformations like rotation, flipping, scaling, cropping, and brightness adjustments to expand the data set. This process improves the performance and robustness of machine learning models, enabling better generalization to real-world variations. Here are some data augmentation techniques used with the CT kidney data set:

1. Rotation: By rotating the image at different angles, we can create new instances of the cyst, stone, normal, and tumor classes.
2. Flipping: Flipping the image horizontally or vertically can also help create new instances of the classes.
3. Scaling: By scaling the image, we can create images of different sizes, which can help create new instances of the minority classes.
4. Adding noise: Adding noise to the image can create new instances of the classes and can also help in making the model more robust to noise in the original images.
5. Elastic deformation: By applying elastic deformation to the image, we can create new instances of the classes that are similar to the original instances but slightly different.
6. Contrast adjustment: Adjusting the contrast of the image can also help create new instances of the classes.

Data augmentation should be applied carefully, and the augmented data set must be validated for its effectiveness in enhancing model performance. When handling medical image data sets, it is crucial to consult a medical professional to ensure that augmentation techniques do not compromise the clinical interpretation of the images. Table 1 shows that data augmentation has significantly increased the number of instances in each class, aiding in data set balance and improving model performance on minority classes. The quantity of new instances generated varies based on the data augmentation techniques and their parameters. Furthermore, the augmented data set must be carefully validated to confirm that it has enhanced the model's performance.

3.3 Image segmentation

CT kidney image segmentation serves a significant role in the analysis of medical images by isolating kidney regions from adjacent tissues. Traditionally, thresholding has been a popular technique for segmentation due to its simplicity and effectiveness. However, this method can be sensitive to noise and may

not always yield precise results. To address these limitations, we pro- pose using Fractional Darwinian Particle Swarm Optimization (FDPSO) for segmentation, which has shown robustness in earlier studies.[18–16]

FDPSO is an optimization algorithm inspired by biological systems, specifically designed for automatic segmentation of kidney regions in CT images. It is a variation of the Particle Swarm Optimization (PSO) algorithm, which simulates the collective behavior of bird flocks or insect swarms. In FDPSO [19, 20], segmentation is achieved by dividing an image into distinct regions based on pixel value similarity.

The FDPSO algorithm operates by leveraging a swarm of particles to seek out the solution space. Each particle represents a possible segmentation solution, and its position and velocity are adjusted based on both its own best position and the best position discovered by the swarm [21]. A distinctive feature of FDPSO is the inclusion of a fractional-order derivative term in the velocity update equation, which improves the algorithm's convergence speed and accuracy [17, 18]. The segmentation process using FDPSO is summarized in the following steps:

1. Defining the objective function: The objective function measures the seg- mentation algorithm's ability to segment renal areas. FODPSO's objective function is the weighted sum of the Dice similarity coefficient (DSC) and the Hausdorff distance (HD). The HD measures the greatest distance between two segments, whereas the DSC measures the overlap between the expected and ground truth segmentations.
2. Initializing the FODPSO algorithm: FODPSO is a population-based optimization method that models particle swarm behavior. The technique begins by randomly initializing a population of particles, with each particle representing a potential solution to the segmentation issue.
3. Evaluating particle fitness: Each particle's fitness is determined using the objective function. The particle's fitness dictates where it appears in the search space.
4. Updating the particles: The particles are updated based on their position and velocity. The particle position represents its current solution to the seg- mentation problem, while its velocity represents its direction of movement in the search space. The updated rules are based on the Darwinian theory of evolution and fractional calculus.
5. Termination: When a stopping criterion is fulfilled, such as a maxi number of iterations or a mini fitness improvement, the FODPSO algorithm terminates.
6. Post-processing: The final segmentation result may need to be post- processed to remove any small or isolated regions and to smooth the boundaries of the kidney regions. Techniques such as morphological operations and Gaussian smoothing can be used for post-processing.

Overall, FODPSO is a powerful optimization algorithm that can automatically segment kidney regions in CT images. There are several advantages of using FODPSO for CT kidney image segmentation over other traditional segmentation techniques:[23 ,22]

1. FODPSO is an optimization algorithm that can automatically search for the optimal segmentation solution in the search space. This means that it does not require manual intervention or parameter tuning, which can save time and improve the reproducibility of the results.
2. FODPSO uses fractional calculus, which is a generalization of traditional calculus that can handle non-integer orders of differentiation and integration. This allows FODPSO to model more complex behaviors and relationships in the image data, which can enhance the accuracy of the segmentation.
3. FODPSO is based on the Darwinian theory of evolution, which simulates natural selection and survival of the fittest. This means that FODPSO can adapt to changes in the image data and converge to the optimal solution robustly and efficiently.
4. FODPSO can be used to optimize multiple objectives simultaneously, such as segmentation accuracy, smoothness, and boundary adherence. This can result in more robust and clinically relevant segmentation results that better reflect the underlying anatomy and physiology.
5. FODPSO has been shown to achieve high accuracy in CT kidney image segmentation. For example, FODPSO achieved a mean Dice similarity coefficient (DSC) of 0.946 and a mean Hausdorff distance (HD) of 8.03 mm in segmenting the kidney regions from CT images.

Overall, FODPSO is a powerful and flexible optimization algorithm that can achieve high accuracy in CT kidney image segmentation. Fig. 3 shows samples of the segmented images using FODPSO

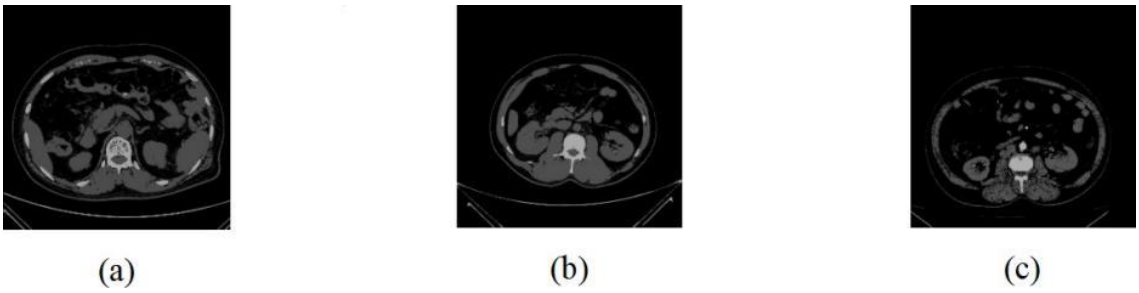

Fig. (3): Samples of the segmented images using FODPSO: (a) Cyst, (b) Kidney Stone, and (c) Tumor

4.1 Feature Extraction

Local Binary Patterns (LBP), Gray level zone length matrix (GLZLM), and Hu Moments are common features that have been commonly used for texture and shape analysis respectively [24]. In the proposed algorithm, we used a com- bination of LBP, Gray level zone length matrix (GLZLM), and Hu Moments along with statistical features as feature descriptors.

3.4.1 Local Binary Pattern

Local Binary Pattern (LBP) is undeniably one of the most prevalent feature descriptors employed in image recognition. LBP is particularly effective in capturing texture details. In the context of gray-scale CT kidney images, LBP can extract information about the texture of local neighborhoods [24].

The primary advantages of LBP are its computational efficiency and robustness to changes in lighting conditions. LBP operates by evaluating the binary relationships between each pixel in the CT kidney image and its neigh- boring pixels. These relationships are encoded into an LBP code according to predefined rules, making it a straightforward yet powerful method for texture analysis.

The pixels imagery gp(p = 0, ..., 7) are labeled by thresholding a 3 by 3 neighborhood of each pixel, with the center pixel value fc and a binary number f (gp − gc) as in Equation (1):

$$f(g_p - g_c) = \begin{cases} 1: g_p \geq g_c \\ 0: otherwise \end{cases} \quad \textbf{(1)}$$

Then, the LBP is calculated as in Equation (2) by assigning a binomial factor 2p for each f (gp − gc):

$$LBP = \sum_{p=0}^{7} f(g_p - g_c)2^p \quad \textbf{(2)}$$

The LBP histogram is often used to depict the statistical distribution of LBP codes. In this scenario, all pixel LBP codes for an input picture are gathered as a texture description into a histogram, which is

$$LBPH(i) = \sum_{x,y} \delta_i, LBP(x,y) \quad i = 0,\ldots,2^7 \quad \textbf{(3)}$$

where the Kroneck product function is denoted by delta(.). To get local texture information, the LBP operator extracts a wide variety of texture primitives, usually aggregated into a histogram across an area, including corner, edge, line end, and spot. The CT kidney image is segmented into many areas, and the LBP feature distributions are then extracted and concatenated to create an enhanced feature vector that may be utilized as a texture descriptor. LBP is a resilient descriptor that can withstand rotation, scaling, background noise, and lighting variations.

3.4.2 Canonical Correlation Analysis

Canonical Correlation Analysis (CCA) is a statistical technique that is used to find linear combinations of two or more sets of variables that have a maximum correlation with each other. In other words, CCA is a method for the measurement of the linear relationship between two multidimensional variables. In the context of feature fusion between Local Binary Patterns (LBP), Gray Level Zone Length Matrix (GLZLM), and Hu Moments, CCA can be used to combine the information contained in these three feature sets into a single set of features with improved discriminatory power. The output of CCA is a set of new features that are linear combinations of the input features and capture the maximum amount of information shared between the different feature sets. These new features can then be used in pattern recognition and classification tasks .

For two random sets f rm1 ×n1 and g rm2 ×n2, a pair of transforma-tions u and v termed canonical transformations are discovered such that the correlation between f′ = utf and g′ = vtg is

maximized. The function to be maximized is specified in Equation4) :

$$r = \frac{E[f^{`},g^{`}]}{\sqrt{E[f^{`2}]E[g^{`2}]}} = \frac{E[u^t f, v^t g]}{\sqrt{E[u^t f\ f^t\ u]E[v^t g\ g^t\ v]}} = \frac{u^t C_{fg} v}{\sqrt{u^t C_{ff}\ u\ v^t\ C_{gg}\ v}} \quad \textbf{(4)}$$

The maximum of r with respect to u and v is the maximum canonical correlation.

$$r = max_{u,v} \frac{u^t C_{fg} v}{\sqrt{u^t C_{ff}\ u\ v^t\ C_{gg}\ v}} \quad \textbf{(5)}$$

r is the canonical correlation. Where $E[h]$ is the expectation of h and C_{ff},

C_{fg} and C_{gg} are covariance matrices

3.4.3 Feature reduction using Two-Dimensional Principal Component Analysis (2DPCA)

Principal Components Analysis (PCA) identifies data patterns and visualizes similarities and contrasts [26]. It is regarded as a good data analysis approach capable of extracting data patterns from high-dimensional data when the use of graphical representation is not possible. The main benefit of PCA is that it compresses data by lowering the number of dimensions while preserving significant information.

For evaluating two-dimensional data, the Two Dimensional PCA (2DPCA) technique outperforms one-dimensional PCA. 2DPCA is more effective in extracting prominent traits, resulting in a higher identification rate. 2DPCA analyzes data in two dimensions while preserving the spatial temporal relationship between surrounding feature components. The 2DPCA's computation stages for a data set are as follows:

- Read the training images of size (X Y), where X and Y denote the number of rows and columns of each image, respectively.
- Calculate the covariance matrix S, according to Equation (6):

$$= \frac{1}{k}\sum_{j=1}^{j=k}(A_{XxYxJ} - \overline{A})^T (A_{XxYxJ} - \overline{A}) \quad \textbf{(6)}$$

Where K is size of the training images, A refer to each training image of the whole K images and $\bar{A}$ is the average matrix of the K images. Figure 4 illustrates that no need to employ all the obtained feature vectors, simply those corresponding to the dominating Eigen vectors. Stack the y dominant Eigen vectors to one projection matrix P = [P1P2P3...Py] of size X × y.

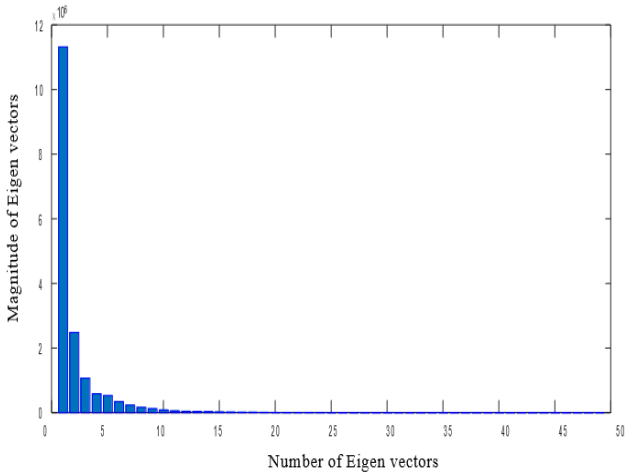

Fig. (4): Obtained Eigen values after 2DPCA

The projection matrix (P) is used to project all the training and testing images to build feature vectors that incorporate only the relevant information of each image. Note that the size of the assessed feature vector is $X \times Y$

In the suggested technique, the generated compact feature descriptors are to be transferred into vector form, and all vectors that belong to the same class are to be aggregated into one matrix representing that class. In the testing phase, all training sets are kept in sequence, where Canonical Correlation Analysis (CCA) is applied to match the testing set to the next training set.

3.5 Classification

Several research have advocated utilizing either SVM [25, 26] or CNN [27, 28] for classifying kidney images. In this research, we offer a hybrid classifier strategy that combines the usage of a binary SVM for quick decision-making with the ability to distinguish between normal and abnormal kidney images. After that, CNN is used to differentiate between various kidney diseases such as tumor, cyst, and stone. Our proposed technique boosted the efficiency and accuracy of renal disease for rapid diagnosis and high accuracy.

3.5.1 First Decision

SVMs use a hyperplane space in a high-dimensional feature space, learned using an optimization theory learning algorithm that incorporates a statistical learning theory learning bias [29, 30]. There are two types of data: training data and testing data. It has been demonstrated that the training data set can generalize and correctly predict new data. Data is mapped in the form of kernels that measure how similar or different data objects are from one another are used to map data. A

classification step involves the identification of which is closely connected to the known classes [31, 32]. The optimal separating hyperplane is obtained by

maximizing the margin between two or more classes of the training data sets.by maximizing the margin between two or more classes. Midway down the margin, this hyperplane has to be minimized.

$$\frac{1}{2}\|W\|^2$$

subject to the constrains yi ((W.Ci + b) ⩾ 1)

Then by optimizing the subsequent Equation (7), the solution of this problem is achieved:

$$\frac{1}{2}\|W\|^2 - \sum_i \propto_i (y_i(\overrightarrow{W}.\overrightarrow{V_i + b) - 1)} \quad \textbf{(7)}$$

where y is the output result, indicating the class label (y ∈ {1,-1} for binary classifier), C is the input feature vectors, and W is the collection of weights, one for each input feature. The points chosen from the input training feature data (C) that meet the maximum margin above and below the hyper- plane [33] are the supported vectors V. A unique maximum margin solution is determined by the output parameters b and α. The chosen support vectors V ′s are represented by the y′s and α′s. Equation (8) defines the decision function d(Q), which is defined for the kernel (K) as follows. It is positive for class 1 and negative for class 2. It predicts the classification of an unknown vector Q.

$$(Q) = sign(\sum_i K(Q, V_i))y_i \propto_i + b \quad \textbf{(8)}$$

Using Binary Support Vector Machine (BSVM) for the initial judgment to classify CT kidney images as normal or abnormal is a prevalent strategy in medical image analysis. Here are the steps involved in utilizing BSVM for this task:

- The data collection of 12,446 CT kidney images has to be splitted into training, validation, and testing sets. This is done to prevent over fitting and to evaluate the effectiveness of the classifier on unknown data.
- Common characteristics for kidney images categorization include intensity-

based features, texture features, and morphological features.

- The BSVM model is trained using the training set of labeled CT kidney images and their related characteristics. The objective is to learn a hyper-plane that can differentiate normal and abnormal images with maximal margin.
- The trained BSVM model is validated using the validation set of labeled CT kidney images. The performance criteria utilized for validation include accuracy, specificity, area under the receiver operating characteristic curve, and sensitivity.
- The resulting BSVM model is evaluated on the testing set of labeled CT kidney images to evaluate its performance on unseen data.

Overall, BSVM is a popular and successful classification strategy for CT kidney images. However, it is crucial to highlight that the performance of BSVM may rely on the choice of hyperparameters and the unique features of the data set.

3.5.2 Second Decision (CNN)

After executing the initial judgment using Binary Support Vector Machine (BSVM) to categorize CT kidney images as normal or abnormal, the next step might be to employ a Convolutional Neural Network (CNN) for further categorization of aberrant images into cysts, stones, and tumors.

A sort of neural network with layers is termed a Convolutional neural network. Grid-structured data are examined, and after that important characteristics are extracted [34]. Employing CNNs have a huge benefit as no considerable pre-processing is necessary. CNNs which is a feed-forward network have been found to give several computational benefits. By mixing both feature extraction and classification, CNN is inspired by biological processes and tries to find patterns directly from images.

A basic Convolutional Neural Network (CNN) comprises four types of layers: convolutional, activation, pooling, and fully-connected layers.

Convolutional layers have distinctive properties: they involve local connections and weight sharing. Each neuron in the input layer connects only to a small, localized region, reflecting the receptive field of the human visual system. This local connectivity means that different neurons respond to different sections of the input, which overlap to form a comprehensive representation of the image. Neurons within a convolutional layer are organized into feature maps, with shared weights across these maps acting as filters. This weight- sharing approach significantly reduces the number of network parameters, enhancing computational efficiency and mitigating over fitting.

To capture more complex features of the input data, convolutional layers are typically followed by non-linear activation layers. Pooling layers are employed to reduce the spatial dimensions of the data by aggregating values within small rectangular regions. Common pooling methods include maximum pooling and average pooling, which replace each region with the maximum or average value, respectively.

Pooling layers help to make the network's output more invariant to minor variations in the input. The network concludes with one or more fully- connected layers, each followed by an activation function, to produce the final classification results. Like traditional artificial neural networks (ANNs), CNNs are trained by minimizing a loss function using gradient descent and back- propagation techniques. Research has shown that hybrid combinations of loss functions, when properly weighted and mixed, often outperform individual loss functions.[37–35]

Deep architectures in CNNs enable learning of data representations at multiple levels of semantic abstraction. This capability allows for the detection of complex visual structures, such as vehicles or faces, in the final layers by combining simpler, low-level features like edges. Designing a deep CNN for specific tasks, however, involves complex algorithmic decisions and numerous interdependent parameter values. While there has been significant progress in deep CNNs for color image classification, there is comparatively less research focused on texture recognition and medical image analysis.[38]

Here are the processes involved in utilizing CNN for this discriminating task:

- CNN architecture needs to be created for categorizing the anomalous images into cysts, stones, and tumors. The design may comprise convolutional layers, pooling layers, dropout layers, and fully linked layers.
- The CNN model is trained using the training set of labeled CT kidney images and their related characteristics. The objective is to discover the traits that may identify between cysts, stones, and tumors with high accuracy.
- The trained CNN model is assessed using the validation set of labeled CT kidney images. The performance criteria utilized for validation include accuracy, precision, recall, and F 1 score.
- The resulting CNN model is evaluated on the testing set of labeled CT kidney images to evaluate its performance on unseen data.

Utilizing CNN for further categorization of aberrant CT kidney images can boost the accuracy of the entire classification process. However, it is crucial to remember that the performance of CNN may rely on the individual properties of the data set and the choice of hyperparameters. It is recommended to tweak the design parameters of CNN to attain the desired enhanced outcomes.

Our suggested model includes a total of 9 layers whose comprehensive description is as follow:

- Input layer:

This layer sets the form of the input data that the model will receive. In this example, it specifies that the input images will have a height and width of 128 pixels, and a single channel for grayscale images or three channels for RGB images.

- Conv2D layer with 32 filters:
  - This layer conducts convolutional filtering on the input images to extract features.
  - It includes 32 filters, each with a size of 3x3 pixels and employs the ReLU activation function to induce non-linearity.
  - The output form of this layer is (126, 126, 32) which implies that the layer creates 32 feature maps of size 126x126.
- MaxPooling 2D layer:
  - This layer conducts pooling operation on the output of the preceding convolutional layer to down sample the feature maps and minimize their spatial dimensions.
  - It employs a pooling size of 2x2 pixels to minimize the height and breadth of the feature maps by a factor of 2.
  - The output form of this layer is (63, 63, 32) which implies that the layer creates 32 feature maps of size 63x63.
- Conv2D layer with 64 filters:
  - This layer conducts another round of convolutional filtering to extract more complicated features from the down sampled feature maps.
  - It includes 64 filters, each with a size of 3x3 pixels and employs the ReLU activation function to induce non-linearity.

  - The output form of this layer is (61, 61, 64) which implies that the layer creates 64 feature maps of size 61x61.

- MaxPooling 2D layer:
  - This layer conducts another pooling operation on the output of the pre- ceding convolutional layer to further down sample the feature maps and minimize their spatial dimensions.
  - It employs a pooling size of 2x2 pixels to minimize the height and breadth of the feature maps by a factor of 2.
  - The output form of this layer is (30, 30, 64) which implies that the layer creates 64 feature maps of size 30x30.

- Conv2D layer with 128 filters:
  - This layer conducts one more round of convolutional filtering to extract even more complicated features from the down sampled feature maps.
  - It has 128 filters, each with a size of 3x3 pixels and employs the ReLU activation function to introduce non-linearity.
  - The output form of this layer is (28, 28, 128) which implies that the layer creates 128 feature maps of size 28x28.

- MaxPooling 2D layer:
  - This layer conducts one additional pooling operation on the output of the preceding convolutional layer to further down sample the feature maps and minimize their spatial dimensions.
  - It employs a pooling size of 2x2 pixels to minimize the height and breadth of the feature maps by a factor of 2.
  - The output form of this layer is (14, 14, 128) which implies that the layer creates 128 feature maps of size 14x14.

- Flatten layer:
  - This layer flattens the output of the previous max pooling layer into a 1D vector.
  - The output shape of this layer is (14x14x128) = 25088 which implies that the layer flattens each of the 128 feature maps of size 14x14 into a vector of length 25088.

- Three thick layers: the first with 512 neurons, second with 256 neurons, and the last output layer with 3 neurons:.

These layers are fully linked layers that take the flattened output of the preceding layer as input and apply a linear transformation on it. It contains 128 neurons and employs a ReLU activation mechanism. The goal of this layer is to execute a non-linear change of the flattened characteristics to make them more appropriate for classification. This is the last output layer of the model that takes the output of the preceding dropout layer as input and performs a linear transformation to it. It has 3 neurons, one for each type of kidney illness, and employs a softmax activation function to output a probability distribution over the categories.

Overall, this model employs a combination of convolutional and dense layers to extract information from the input picture and perform classification. The inclusion of dropout layers helps to prevent over fitting, while the softmax activation function in the output layer allows the model to output a probability distribution over the categories.

4 Experimental Setup

4.1 Utilized Data set

The data set was sourced from the Picture Archiving and Communication System (PACS) across multiple hospitals in Dhaka, Bangladesh. These hospitals provided images from individuals who had been diagnosed with various kidney conditions, including normal, cysts, tumors, or stones.[39]

The data set includes Coronal and Axial slices obtained from both contrast and non-contrast examinations of the abdomen and urogram. For each diagnosis, DICOM studies were meticulously selected to develop a batch of images focused on the region of interest corresponding to each radiological finding. These DICOM images were then converted to a lossless JPEG format, with all patient information and metadata removed to ensure privacy.

Subsequent to conversion, each image was reviewed again by both a radiologist and a medical technician to verify the accuracy of the data. The final data set consists of 12,446 unique images, categorized as follows: 3,709 images of cysts, 5,077 images of normal kidneys, 1,377 images of stones, and 2,283 images of tumors.

4.2 Implementation Details

The LBP feature vector captures the overall description of an x-ray renal image via the concatenation of local histograms. The user determines the concatenation of the histogram, but it should be consistent across all photos. The LBP feature vector is very large; for example, given a 256x256 pixel image, a sub-block size of 16x16, and uniform LBP, the feature space is 944 dimensions. We segmented the picture into non-overlapping 16x16 pixel zones and then calculated the number of zones in each image. The picture size is 256x256, and each zone is 16x16, yielding (256/16) × (256/16) = 16 x 16 = 256 zones. Because GLZLM extracts one feature per zone, the feature vector size was 256. Hu Moments typically generate a constant set of seven characteristics, regardless of image size.

- X1= LBP: 944 x1
- X2= GLZLM: 256 x1
- X3= Hu Moments: 7 x1

To stack them together, we concatenated the feature vectors in the following order: LBP, GLZLM, Hu Moments. The feature vectors are aligned appropriately for stacking. the second feature vector (X2) with size 256 x 1 will be placed vertically below the first feature vector (X1) with size 944 x 1, and then the third feature vector (X3) with size 7 x 1 will be layered below them. The resulting stacked features vector will have a dimension of 1207 x 1 .

CCA (Canonical Correlation Analysis) is a multivariate statistical approach that may integrate or fuse several feature vectors into a single vector representation. The integration is performed by finding linear combinations of the original feature vectors that optimize the correlation between them. The result of CCA would be a new set of canonical variables, which reflect the integrated characteristics. The number of canonical variables obtained would depend on the size of the original feature vectors and the correlations between them. the original feature vectors have dimensions 944x1, 256x1, and 7x1, the resultant integrated feature vector after applying CCA will be 400 x1. It's vital to note that the integration of features using CCA tries to capture the

common information and correlations across the feature sets.

By using 2D PCA to the 400 x1 feature vector, we have successfully decreased the dimensionality to 100, allowing for simpler visualization and perhaps collecting the most relevant information in the data. The output feature 100 x1 per each image

4.3 Evaluation Metrics

Disease classification performance is evaluated using the output of a binary or multi-class classifier. To demonstrate our proposal's good performance, many assessment criteria were used, including sensitivity, accuracy, specificity, and precision.

The sensitivity

It assesses the accuracy of positive cases by determining how many positive samples were accurately identified. This is expressed in Equation (9), where TP stands for true positives (properly discovered occurrences) and FN for false negatives (positive cases misclassified as negative).

$$Sensitivity\ (Recall)\ = \frac{TP}{TP + FN} \qquad \textbf{(9)}$$

Accuracy

It is used to assess categorization performance. It estimates the proportion of samples that are categorized properly, as indicated in Equation (10).

$$Accuracy\ = \frac{TP + TN}{TP + FN - FP + FN} \qquad \textbf{(10)}$$

Specificity

Equation (11) refers to the conditional probability of true negatives given a secondary class.

$$Specificity\ = \frac{TN}{TN + FP} \qquad \textbf{(11)}$$

Precision

Equation (12) calculates it as the number of true positives divided by the total of true positives and false positives. It assesses the algorithm's prediction capacity. Precision relates to how "accurate" the model is in terms of how many expected positives are genuinely positive.

$$Precision\ = \frac{TP}{TP + FP} \qquad \textbf{(12)}$$

F-score

It evaluates the positive class by combining precision and recall, as illustrated in Equation (13). A high number suggests higher model performance on the positive class.

$$F_{\ score}\ = \ 2\ *\ \frac{Precision * Recall}{Precision + Recall} \qquad \textbf{(13)}$$

5 RESULTS AND DISCUSSION

The binary SVM model's performance was evaluated using a data set of 35,163 CT kidney images. We trained the model to classify instances as 'Abnormal' or 'Normal' and assessed its performance with a confusion matrix. The used data set was separated into training and testing sets. Here, we'll employ an 80/20 split (80% for training and 20% for testing). First, we'll determine the amount of samples for each class in the training and testing sets based on the 80/20 split as follow:

Training Set:

Normal: 80% of 14,308 = 11,446 samples

Abnormal (Cyst, Stone, Tumor): 80% of (10,527 + 3,885 + 6,443) = 16,684 samples

Testing Set:

Normal: 20% of 14,308 = 2,862 samples

Abnormal (Cyst, Stone, Tumor): 20% of (10,527 + 3,885 + 6,443) = 4,171 samples

The model scored flawlessly in both classes, resulting in 100% accuracy overall. This suggests that the model accurately classified all instances, which is impressive for a binary classification task. The high accuracy demonstrates the binary SVM model's effectiveness in correctly diagnosing medical diseases, which is critical in the context of medical diagnosis and therapy.

Table (2:) Experimental results comparing our proposed against recent state of the art techniques

Method	Year	Data size	Achieved accuracy %
CNN [40]	2019	315	83
Inception V3 [41]	2020	192	97
XGBoost [42]	2020	177	77
AdaBoost [43]	2020	735	75
2D CNN [44]	2022	8400	97
Ours	2024	35163	99.9

Additional research and assessment on various data sets and tasks are required to determine the model's generalization capacity. The binary SVM model's performance is assessed using 5-fold cross-validation. The data set was randomly divided into five subgroups of roughly similar size, each with an equal percentage of 'Abnormal' and 'Normal' instances. We trained the binary SVM model on four subgroups and tested it on the remaining subset before repeating the process for all possible subset combinations. The model achieved a perfect score on all five folds cross validation sets, resulting in an average accuracy of 100% with a standard deviation of 0.0%. These findings show that the binary SVM model is both robust and generalizable, and that it can accurately classify medical abnormalities in CT kidney images.

The binary SVM model constantly performs well across the data set, as seen by its 100% accuracy in all five folds cross validation subgroups. Following the first judgment using BSVM to categorize CT kidney pictures as normal or abnormal, the next step is to use a Convolutional Neural Network (CNN) to further categorize aberrant images into cysts, stones, and tumors. Figure 5 depicts the confusion matrix for anomalous occurrences (Cyst, Stone, and Tumor) classification. Figure 6 shows the accuracy, recall, and F1 scores for each class. Precision is the proportion of genuine positive forecasts among all positive forecasts, whereas recall is the proportion of true positive predictions among all real positive cases. The F1 score is calculated as the harmonic mean of accuracy and recall, giving equal weight to both measures.

The model performed well across all classes, achieving excellent accuracy and recall. This indicates its effectiveness in correctly identifying class instances while minimizing false positives and negatives. The findings demonstrate high accuracy, recall, and F1-scores for all three classes (Cyst, Stone, and Tumor), indicating effective detection by the model. Both the macro and weighted average F1-scores are similarly robust, reflecting strong overall performance. Additionally, the high accuracy score suggests the model identified 99.9% of the samples in the data set accurately. The findings in Table 2 show that our proposal surpasses other state-of- the-art methods.

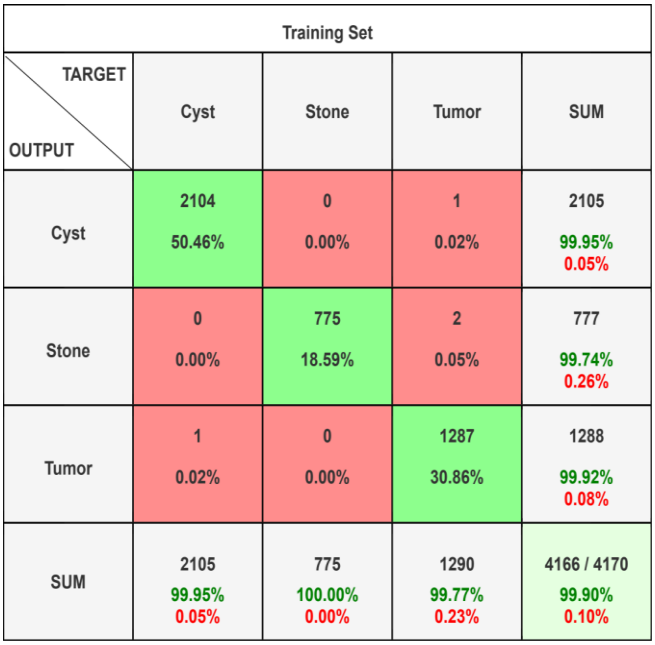

Fig. (5): Confusion matrix for Abnormal instances (Cyst, Stone, and Tumor)

The impressive results from our proposal stem from combining various machine learning methods, including BSVM, CNN, LPB, GLZM, and Hu moment, which enhance model performance. Below is a brief overview of each method's contribution to the model's effectiveness:

- Employing the supervised learning method known as BSVM (Binary Sup- port Vector Machine) to classify data into one of two categories can handle enormous volumes of data and is noted for its ability to generalize effectively.
- Our CNN was intended to automatically find robust characteristics in images

for improved identification of important aspects in the images boosting its ability to categorize them appropriately.

- Local Binary Pattern (LBP) that calculates the texture of an image by

comparing the intensity of each pixel with its surrounding pixels was utilized as one of the used feature descriptors in our suggested.

- Gray Level Co-occurrence Matrix (GLZM) is another feature extraction

approach used in image processing. It estimates the incidence of pairs of pixel intensities in a picture. By employing GLZM, the model was able to gather more information about the textures of the images, which can be valuable for categorization.

Class Name	Precision	1-Precision	Recall	1-Recall	f1-score
Cyst	0.9995	0.0005	0.9995	0.0005	0.9995
Stone	0.9974	0.0026	1.0000	0.0000	0.9987
Tumor	0.9992	0.0008	0.9977	0.0023	0.9984
Accuracy	0.9990				
Misclassification Rate	0.0010				
Macro-F1	0.9989				
Weighted-F1	0.9990				

Fig. (6): Performance measures for Abnormal instances (Cyst, Stone, and Tumor)

In addition to the texture-based feature descriptors, Hu moment which is a set of mathematical characteristics for form analysis was applied. It was used to describe the form of an item in a photograph. By employing Hu moment, the model may be able to collect extra information on the forms of the objects in the images.

By integrating these strategies, our model leveraged the strengths of each methodology and enhanced its image classification capacity through CCA, effectively combining the complementary performance of each descriptor.

The use of 2DPCA effectively preserves dominant features while eliminating redundant ones, positively impacting computational complexity and runtime, as shown in Figure 7. This figure compares the time efficiency of our method with current strategies across all three classes (Cyst, Stone, and Tumor), demonstrating that our approach achieves the lowest runtime and fastest results.

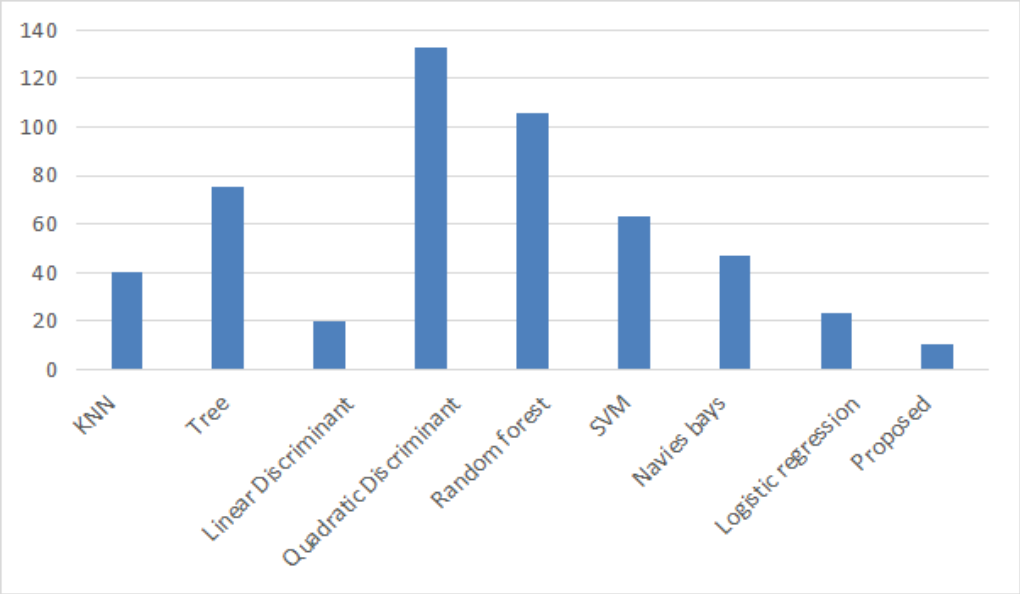

Fig. (7): Time comparison between the proposed and most recent techniques over all three classes (Cyst, Stone, and Tumor))

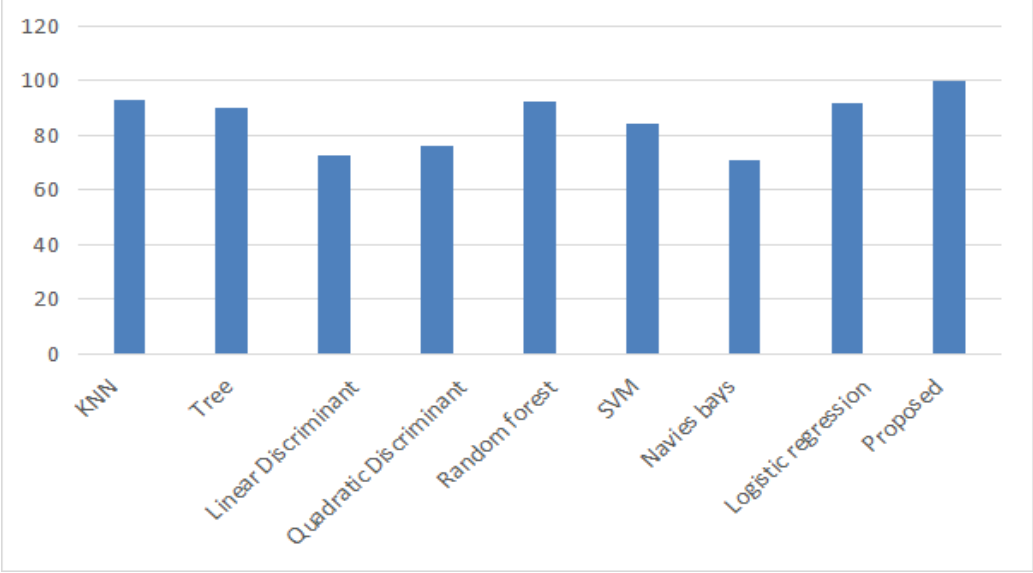

Fig. (8): The accuracy comparison between our proposed and classical machine learning techniques over all three classes (Cyst, Stone, and Tumor)

Figure 8 compares our proposed machine learning strategies with conventional methods across all three classes (Cyst, Stone, and Tumor) based on accuracy. Our approach achieved the highest performance, reaching an accuracy of 99.9%.

Table (3): The comparison between the proposed and most recent classical machine learning in Cyst class.

Method	Precision	Recall	F1 Score
KNN	0.931	0.943	0.937
Tree	0.925	0.953	0.939
Linear Discrimination	0.814	0.835	0.824
Quadratic Discriminant	0.835	0.865	0.850
Random Forest	0.937	0.949	0.943
SVM	0.867	0.888	0.877
Navies Bayes	0.815	0.656	0.727
Logistic Regression	0.923	0.911	0.917
Our Proposed	0.9995	0.9995	0.9995

Table (4): The comparison between the proposed and most recent classical machine learning in Stone class.

Method	Precision	Recall	F1 Score
KNN	0.916	0.922	0.919
Tree	0.873	0.841	0.857
Linear Discrimination	0.699	0.635	0.665
Quadratic Discriminant	0.707	0.716	0.711
Random Forest	0.911	0.919	0.915
SVM	0.738	0.765	0.751
Navies Bayes	0.687	0.631	0.658
Logistic Regression	0.901	0.909	0.905
Our Proposed	0.9974	1	0.9987

Tables 3, 4, and 5 compare the performance of our proposed approach with various classical machine learning techniques for individual classes (Cyst, Stone, and Tumor). Clearly, our method outperformed all classical techniques for each class.

6 CONCLUSIONS

In this work we presented our suggested strategy leveraging AI approaches to improve the identification and classification of kidney diseases in CT images. Our two-step decision technique has obtained exceptional results with a binary

Table (5): The comparison between the proposed and most recent classical machine learning in Tumor class.

Method	Precision	Recall	F1 Score
KNN	0.928	0.929	0.928
Tree	0.888	0.859	0.873
Linear Discrimination	0.714	0.714	0.714
Quadratic Discriminant	0.751	0.748	0.749
Random Forest	0.925	0.934	0.929
SVM	0.789	0.792	0.790
Navies Bayes	0.712	0.699	0.705
Logistic Regression	0.920	0.919	0.919
Our Proposed	0.9992	0.9977	0.9984

accuracy of 100 % to differentiate between normal and abnormal kidney images. The ultimate discriminating judgment between three renal diseases was made with accuracy score of 99.9%. The strategy employs a mix of an efficient Image pre-processing, segmentation, feature extraction, and fusion approaches. Classification was carried out utilizing a two-step classification strategy combining both SVM and CNN. Compared to previous approaches published in the literature, the suggested strategy has attained greater accuracy ratings. The results show that the proposed technique has the potential to boost kidney disease detection and classification efficiency and accuracy, and helping doctors in their clinical practice.

REFERENCES

[1] Malik, P., Pathania, M., Rathaur, V.K., *et al.*: Overview of artificial intel- ligence in medicine. Journal of family medicine and primary care **8**(7), 2328 (2019)

[2] S. Tripathy, S.N. R. Sivakumar, Inbamalar, T.M.: Analysis and detection of nephrolithiasis using imaging techniques. International Journal of Biology and Biomedical Engineering **15**, 3646 (2021)

[3] AKSAKALLI, I., KAC¸ DIOG˘ LU, S., HANAY, Y.S.: Kidney x-ray images classification using machine learning and deep learning methods. Balkan Journal of Electrical and Computer Engineering **9**(2), 144–151 (2021)

[4] Burlacu, A., Iftene, A., Jugrin, D., Popa, I.V., Lupu, P.M., Vlad, C., Covic, A.: Using artificial intelligence resources in dialysis and kidney transplant patients: a literature review. BioMed Research International **2020** (2020)

[5] Vankdothu, R., Hameed, M.A.: Brain tumor segmentation of mr images using svm and fuzzy classifier in machine learning. Measurement: Sensors **24**, 100440 (2022)

[6] Sumana, G., Babu, G.A.: Prediction of nephrolithiasis based on extracted features of ct-scan images using artificial neural networks. International Journal of Advanced Research in Computer Science **8**(5) (2017)

[7] Park, S., Park, B.S., Lee, Y.J., Kim, I.H., Park, J.H., Ko, J., Kim, Y.W., Park, K.M.: Artificial intelligence with kidney disease: A scoping review with bibliometric analysis, prisma-scr. Medicine **100**(14) (2021)

[8] Dritsas, E., Trigka, M.: Machine learning techniques for chronic kidney disease risk prediction. Big Data and Cognitive Computing **6**(3), 98 (2022)

[9] Baidya, D., Umaima, U., Islam, M.N., Shamrat, F.J.M., Pramanik, A., Rahman, M.S.: A deep prediction of chronic kidney disease by employing machine learning method. In: 2022 6th International Conference on Trends in Electronics and Informatics (ICOEI), pp. 1305–1310 (2022). IEEE

[10] Vaish, P., Bharath, R., Rajalakshmi, P., Desai, U.B.: Smartphone based automatic abnormality detection of kidney in ultrasound images. In: 2016 IEEE 18th International Conference on e-Health Networking, Applica- tions and Services (Healthcom), pp. 1–6 (2016). IEEE

[11] Verma, J., Nath, M., Tripathi, P., Saini, K.: Analysis and identification of kidney stone using k th nearest neighbour (knn) and support vector machine (svm) classification techniques. Pattern Recognition and Image Analysis **27**, 574–580 (2017)

[12] Chaitanya, S., Rajesh Kumar, P.: Classification of kidney images using cuckoo search algorithm and artificial neural network. Int J Eng Adv Technol **8**(3), 370–374 (2019)

[13] Kim, D.-H., Ye, S.-Y.: Classification of chronic kidney disease in sonogra- phy using the glcm and artificial neural network. Diagnostics **11**(5), 864 (2021)

[14] Ifraz, G.M., Rashid, M.H., Tazin, T., Bourouis, S., Khan, M.M., et al.: Comparative analysis for prediction of kidney disease using intelligent machine learning methods. Computational and Mathematical Methods in Medicine **2021** (2021)

[15] N. A. Lakshmi, M.S.A.S. B. Jyothirmayi, Santoshi, G.: Kidney stone detection from ultrasound images by using canny edge detection and cnn classification. International Journal for Research in Engineering Application Management (IJREAM) **05** (2020)

[16] Kumar, A.S., Kumar, A., Bajaj, V., Singh, G.K.: Fractional-order darwinian swarm intelligence inspired multilevel thresholding for mammogram segmentation. In: 2018 International Conference on Communication and Signal Processing (ICCSP), pp. 0160–0164 (2018). IEEE

[17] Ghamisi, P., Couceiro, M.S., Ferreira, N.M., Kumar, L.: Use of darwinian particle swarm optimization technique for the segmentation of remote sensing images. In: 2012 IEEE International Geoscience and Remote Sensing Symposium, pp. 4295–4298 (2012). IEEE

[18] Ahilan, A., Manogaran, G., Raja, C., Kadry, S., Kumar, S.N., Kumar, C.A., Jarin, T., Krishnamoorthy, S., Kumar, P.M., Babu, G.C., *et al.*: Segmentation by fractional order darwinian particle swarm optimization based multilevel thresholding and improved lossless prediction-based compression algorithm for medical images. Ieee Access **7**, 89570–89580 (2019)

[19] Elaraby, W.S., Madian, A.H.: Meta-heuristic optimization algorithms for irradiated fruits and vegetable image detection. WSEAS Transactions on Computers **20**, 118–130 (2022)

[20] Dumitru, D., Dios, an, L., Andreica, A., B´alint, Z.: A transfer learning approach on the optimization of edge detectors for medical images using particle swarm optimization. Entropy **23**(4), 414 (2021)

[21] Tillett, J., Rao, T., Sahin, F., Rao, R.: Darwinian particle swarm optimization (2005)

[22] Mohsin, A.H., Zaidan, A., Zaidan, B., Albahri, O., Albahri, A., Alsalem, M., Mohammed, K., Nidhal, S., Jalood, N.S., Jasim, A.N., *et al.*: New method of image steganography based on particle swarm optimization algorithm in spatial domain for high embedding capacity. IEEE Access **7**, 168994–169010 (2019)

[23] Couceiro, M.S., Rocha, R.P., Ferreira, N.F., Machado, J.T.: Introducing the fractional-order darwinian pso. Signal, Image and Video Processing **6**(3), 343–350 (2012)

[24] Humeau-Heurtier, A.: Texture feature extraction methods: A survey. Ieee Access **7**, 8975–9000 (2019)

[25] Chang, C.-C., Lin, C.-J.: Libsvm: a library for support vector machines ACM transactions on intelligent systems and technology (TIST) **2**(3), 1–27 (2011)

[26] Sester, J., Hayes, D., Scanlon, M., Le-Khac, N.-A.: A comparative study of support vector machine and neural networks for file type identi- fication using n-gram analysis. Forensic Science International: Digital Investigation **36**, 301121 (2021)

[27] LeCun, Y., Bengio, Y., Hinton, G.: Deep learning. nature **521**(7553), 436– 444 (2015)

[28] Krizhevsky, A., Sutskever, I., Hinton, G.E.: Imagenet classification with deep convolutional neural networks. Communications of the ACM **60**(6), 84–90 (2017)

[29] Zhang, Y.: Support vector machine classification algorithm and its application. In: Information Computing and Applications: Third Interna- tional Conference, ICICA 2012, Chengde, China, September 14-16, 2012. Proceedings, Part II 3, pp. 179–186 (2012). Springer

[30] Pisner, D.A., Schnyer, D.M.: Support vector machine. In: Machine Learning, pp. 101–121. Elsevier, (2020)

[31] McCoubrey, L.E., Elbadawi, M., Orlu, M., Gaisford, S., Basit, A.W.: Har- nessing machine learning for development of microbiome therapeutics. Gut Microbes **13**(1), 1872323 (2021)

[32] Brnabic, A., Hess, L.M.: Systematic literature review of machine learning methods used in the analysis of real-world data for patient-provider deci- sion making. BMC medical informatics and decision making **21**(1), 1–19 (2021)

[33] Cervantes, J., Garcia-Lamont, F., Rodr´ıguez-Mazahua, L., Lopez, A.: A comprehensive survey on support vector machine classification: Applica- tions, challenges and trends. Neurocomputing **408**, 189–215 (2020)

[34] Saad, M.H., Hashima, S., Sayed, W., El-Shazly, E.H., Madian, A.H., Fouda, M.M.: Early diagnosis of covid-19 images using optimal cnn hyperparameters. Diagnostics **13**(1), 76 (2023)

[35] Jiang, J., El-Shazly, E.H., Zhang, X.: Gaussian weighted deep modeling for improved depth estimation in monocular images. IEEE Access **7**, 134718– 134729 (2019)

[36] El-Shazly, E.H., Zhang, X., Jiang, J.: Improved appearance loss for deep estimation of image depth. Electronics Letters **55**(5), 264–266 (2019)

[37] El-Shazly, E.H., Abdelhakim, A., Zhang, X., Fares, A.: Non-linear integration of loss terms for improved new view synthesis. Multimedia Tools and Applications, 1–18 (2023)

[38] Rhee, E.J., *et al.*: A deep learning approach for classification of cloud image patches on small data sets. Journal of information and communication convergence engineering **16**(3), 173–178 (2018)

[39] Islam, M.N., Hasan, M., Hossain, M.K., Alam, M.G.R., Uddin, M.Z., Soylu, A.: Vision transformer and explainable transfer learning models for auto detection of kidney cyst, stone and tumor from ct-radiography. Scientific Reports **12**(1), 11440 (2022)

[40] Zhou, L., Zhang, Z., Chen, Y.-C., Zhao, Z.-Y., Yin, X.-D., Jiang, H.- B.: A deep learning-based radiomics model for differentiating benign and malignant renal tumors. Translational oncology **12**(2), 292–300 (2019)

[41] Zabihollahy, F., Schieda, N., Krishna, S., Ukwatta, E.: Automated classi- fication of solid renal masses on contrast-enhanced computed tomography images using convolutional neural network with decision fusion. European Radiology **30**, 5183–5190 (2020)

[42] Schieda, N., Nguyen, K., Thornhill, R.E., McInnes, M.D., Wu, M., James, N.: Importance of phase enhancement for machine learning classification of solid renal masses using texture

analysis features at multi-phasic ct. Abdominal Radiology **45**, 2786–2796 (2020)

[43] Yap, F.Y., Varghese, B.A., Cen, S.Y., Hwang, D.H., Lei, X., Desai, B., Lau, C., Yang, L.L., Fullenkamp, A.J., Hajian, S., *et al.*: Shape and texture-based radiomics signature on ct effectively discriminates benign from malignant renal masses. European radiology **31**, 1011–1021 (2021)

[44] Alzu'bi, D., Abdullah, M., Hmeidi, I., AlAzab, R., Gharaibeh, M., El-Heis, M., Almotairi, K.H., Forestiero, A., Hussein, A.M., Abualigah, L.: Kidney tumor detection and classification based on deep learning approaches: a new data set in ct scans. Journal of Healthcare Engineering **2022**, 1–22 (2022).